Vaccination with *ENO1*-DNA Prolongs Survival of Genetically Engineered Mice with Pancreatic Cancer

PAOLA CAPPELLO[1,2], SIMONA ROLLA[1,2], ROBERTO CHIARLE[1], MOITZA PRINCIPE[1,2], FEDERICA CAVALLO[2,3], GIOVANNI PERCONTI[4,5], SALVATORE FEO[4,5], MIRELLA GIOVARELLI[1,2], FRANCESCO NOVELLI[1,2].

[1]Center for Experimental Research and Medical Studies (CERMS), Città della Salute e della Scienza di Torino, and [2]Department of Molecular Biotechnology and Health Science, University of Torino, 10125 Torino, Italy; [3]Molecular Biotechnology Center, University of Torino, 10126 Turin, Italy; [4]Department of Experimental Oncology and Clinical Applications, University of Palermo, and [5]Institute of Biomedicine and Molecular Immunology, National Council of Research, 90100 Palermo, Italy.

Short title: DNA vaccination delays PDA progression

This work was supported by the Associazione Italiana per la Ricerca sul Cancro (AIRC IG n.11643, 5 x 1000 n.12182); Ministero dell'Istruzione, dell'Università e della Ricerca (MIUR), Progetti di Rilevante Interesse Nazionale (PRIN); Ministero della Sanità: Progetto Integrato Oncologia; Regione Piemonte: Ricerca Industriale e Sviluppo Precompetitivo (ONCOPROT), Ricerca Industriale "Converging Technologies" (BIOTHER), Progetti strategici su tematiche di interesse regionale o sovra regionale (IMMONC), Ricerca Sanitaria Finalizzata, Ricerca Sanitaria Applicata; European Community, European Community's Seventh Framework Programme (FP7/2007-

2013) under Grant agreement n°256974. P.C. was supported by a fellowship from Fondazione Italiana Ricerca sul Cancro (FIRC).

Abbreviations: ENO1, alpha-enolase; CDC, complement-dependent cytotoxicity; GEM, genetically engineered mice; KC, $Kras^{G12D}$/Cre mice; KPC, $Kras^{G12D}$/$Trp53^{R172H}$/Cre mice; MDSC, myeloid-derived suppressor cells; PDA, pancreatic ductal adenocarcinoma; Treg, T regulatory lymphocytes

Correspondence: Francesco Novelli, PhD, CeRMS-University of Turin, Via Cherasco 15 10125-Torino, Italy. Phone: +39 011 6334463, Fax: +39 011 633 6887, Email: franco.novelli@unito.it

Competing interest statement: The authors declare that they have no competing financial interests.

Authors' Contributions: PC designed experiments, acquired, analyzed data and wrote the paper; SR acquired and analyzed data; RC analyzed all histological samples; FC provided the electroporator instrument, as well as valuable scientific comments; MP performed the CDC experiments; GP and SF provided ENO1 full-length coding plasmids and expertise in protein purification; MG helped to design experiments; FN supervised the study, obtained funds and revised the paper.

Abstract

BACKGROUND & AIMS: Pancreatic ductal adenocarcinoma (PDA) is an aggressive tumor, and patients typically present with late-stage disease; rates of 5-year survival after pancreaticoduodenectomy are low. Antibodies against α-enolase (ENO1), a glycolytic enzyme, are detected in more than 60% of patients with PDA, and ENO1-specific T cells inhibit the growth of human pancreatic xenograft tumors in mice. We investigated whether an *ENO1* DNA vaccine elicits anti-tumor immune responses and prolongs survival of mice that spontaneously develop autochthonous, lethal pancreatic carcinomas.

METHODS: We injected and electroporated a plasmid encoding ENO1 (or a control plasmid) into $Kras^{G12D}$/Cre mice (KC) and $Kras^{G12D}$/$Trp53^{R172H}$/Cre (KPC) mice when they were 4 weeks old (when pancreatic intraepithelial lesions are histologically evident). Anti-tumor humoral and cellular responses were analyzed by histology, immunohistochemistry, ELISAs, flow cytometry, and ELISpot and cytotoxicity assays. Survival was analyzed by Kaplan-Meier analysis.

RESULTS: The ENO1 vaccine induced antibody and a cellular responses and increased survival times by a median 138 days in KC mice and 42 days in KPC mice, compared with mice given the control vector. In histologic analysis, the vaccine appeared to slow tumor progression. The vaccinated mice had increased serum levels of anti-ENO1 immunoglobulin G, which bound the surface of carcinoma cells and induced complement-dependent cytotoxicity. ENO1 vaccination reduced numbers of myeloid-derived suppressor cells and T-regulatory cells, and increased T-helper 1 and 17 responses.

CONCLUSIONS: In a genetic model of pancreatic carcinoma, vaccination with *ENO1* DNA elicits humoral and cellular immune responses against tumors, delays tumor progression, and significantly extends survival. This vaccination strategy might be developed as a neo-adjuvant therapy for patients with PDA.

KEYWORDS: Th17, IFNγ, anti-tumor immunity; immunotherapy; IgG-mediated CDC

Introduction

Pancreatic ductal adenocarcinoma (PDA) is the fourth leading cause of cancer-related death in the Western countries. Surgical resection is the only potentially curative treatment. Unfortunately, because of the late presentation of the disease, only 15-20% of patients are candidates for pancreatectomy. However, the five-year survival following pancreaticoduodenectomy is only 25-30% for node-negative, and 10% for node-positive tumors [1, 2]. Effective diagnostic and therapeutic strategies are still urgently needed to improve this survival rate. We have used SERological Proteome Analysis to identify a dozen antigens expressed by PDA and recognized by autoantibodies present in the sera of patients with pancreatic cancer, but not in sera of other tumor patients, patients with pancreatitis or healthy donors [3]. One of these antigens, α-enolase (ENO1), is specifically recognized by over 60% of PDA patients [4]. ENO1 is coded by the *ENO1* gene, is overexpressed in the cytoplasm of PDA cells and is also present on their membrane [5]. In the cytoplasm, ENO1 acts as a glycolytic enzyme, whereas on the membrane it acts as a plasminogen receptor and plays an important role in cell migration [6, 7]. We have shown that PDA patients with autoantibodies to ENO1 also present an ENO1-specific T cell response, which is not observed in patients with no ENO1 autoantibodies. Upon transferral into immunocompromised mice, ENO1-specific T cells inhibit the growth of xenotransplanted human pancreatic tumors. Despite the ubiquitous presence of ENO1 in all mammalian cells, normal cells expressing low levels of ENO1, are spared by ENO1-specific cytotoxic T lymphocytes [5].

In this work, we used two GEM strains ($Kras^{G12D}$/Cre mice, KC mice, and $Kras^{G12D}$/$Trp53^{R172H}$/Cre, KPC mice) that develop autochthonous lethal pancreatic carcinomas with different kinetics [8, 9] in order to study the protective effect of a DNA vaccine to human ENO1.

Mice were vaccinated with plasmids encoding human ENO1 as it displays more than 95% identity (99% homology) with the mouse ortholog. Vaccination, starting from 4 weeks of age, when pancreatic intraepithelial lesions are already histologically evident [8] elicits an integrated humoral and cellular immune response to ENO1

that significantly extends survival. Our data also show a new role of ENO1 in skewing the T cell response toward a Th17-type response. ENO1 vaccination may therefore be a promising neo-adjuvant form of PDA management.

Material and Methods

***Mice*.**

Mice carrying single-mutated $Kras^{G12D}$ (C57BL/6;129SvJae H-2^{b}) or double-mutated ($Kras^{G12D}$ and $Trp53^{R172H}$) (129SvJae H-2^{b}) under the endogenous promoter and flanked by Lox-STOP-Lox cassettes were obtained from Dr. David Tuveson (Cancer Research UK, Cambridge Research Institute, Cambridge, UK). C57BL/6 mice expressing Cre recombinase under a specific pancreatic transcriptional factor Pdx-1 (pancreatic duodenum homeobox 1) promoter were obtained from Dr. Andrew Lowy (University of San Diego, San Diego, CA). Mice were bred and maintained under SAPF conditions at the animal facilities of the Molecular Biotechnology Center, and treated in accordance with EU and Institutional guidelines. Pancreatic cancer -prone KC and KPC mice were generated by crossing single-mutated $Kras^{G12D}$ or double-mutated $Kras^{G12D}$ and $Trp53^{R172H}$ with C57BL/6 mice expressing Cre recombinase. Mice were screened by PCR using tail DNA amplified by specific primers to the Lox-P cassette flanking *Kras* and wild-type *Kras* genes, the Lox-P cassette flanking *Trp53* mutated and wild-type *Trp53* and *Cre* recombinase genes. PCR products were separated on 1.5% agarose gels with GelRed (Biotum by SIC, Rome, Italy) and recorded as .tiff.

DNA Vaccination

KC and KPC mice were vaccinated at 4 weeks of age and every 3 weeks, for a total of three rounds of vaccination, or every 2 weeks, and for a total of four rounds of vaccination. In the therapeutical DNA vaccination setting, KC mice were vaccinated at 32-36 weeks of age and every 3 weeks, for a total of three rounds of vaccination. Injection of 50 μg of plasmid in 40 μl of sterile water with 0.9% NaCl into the femoral muscle of mice anesthetized with Zoletil e Xylazina was immediately followed by two 25 msec pulses of 375 V/cm applied with a CLINIPORATOR™ and linear needle electrodes (IGEA, Carpi, Italy). KC and KPC mice of the same age were randomly assigned to control and treatment groups, and all groups were specifically treated

concurrently. Mice were monitored weekly and left to live unless showing obvious signs of pain, so as to obtain a Kaplan-Meier survival curve. Parallel mice were sacrificed at 4, 24 and 36 weeks of age as indicated, to perform histological or immunohistochemical analyses.

Human *ENO1* cDNA was obtained by enzyme digestion of the plasmid pRC-*ENO1* [10] (kindly provided by Giallongo A, Institute of Biomedicine and Molecular Immunology, National Council of Research, Palermo, Italy) in HindIII and XbaI restriction sites (both from M-Medical, Milan, Italy), followed by separation by electrophoresis on agarose gel and elution. It was then cloned into pVAX1 (Invitrogen, Milan, Italy), previously digested with the same restriction enzymes, by ligation. In order to propagate and maintain empty and pVAX-*ENO1* vectors, the competent *rec*A1, *end*A *E. coli* strain (TOP10) was transformed with the empty pVAX and ligation mixture, and selected on Luria Bertoni plates containing 50 μg/ml kanamycin.

Cells

Syngeneic murine DT6606 and K8484 cells were kindly provided by Dr K. Olive (Li Ka Shing Centre, Cambridge Research Institute, Cancer Research UK, Cambridge, UK). They were obtained from a $Kras^{G12D}$/Cre and a $Kras^{G12D}$/$Trp53^{R172H}$/Cre pancreatic tumor mass, respectively, and were maintained *in vitro* in DMEM-10% FBS.

ELISA. Anti-ENO1 IgG were measured by ELISA by binding to human rENO1 (1.5 μg/ml in Na_2CO_3 0.1M), produced as previously described [5]. Sera collected 2 weeks after three rounds of vaccination were diluted 1:500 in PBS and antibody concentration was calculated by regression analysis using eight two-fold serial dilutions of 1μg/ml of 72/1.11 mAb for a standard curve (kindly provided by P. Migliorini, University of Pisa, Italy).

Serum-binding potential.

Sera from untreated and empty or *ENO1*-vaccinated mice were used to stain DT6606 or K8484 cells, which were analyzed by flow cytometry after dilution of 1:50. Briefly, 1 x 10^5 cells were washed with PBS-0.2% BSA-0.01% NaN_3, and incubated with diluted sera for 1h at 4°C. After two washes, cells were incubated with an APC-conjugated anti-mouse antibody (1:200; Biolegend) for 30 min on ice. Following washing, 10,000 cells were acquired with a FACSCanto using CellQuest software (both BD Biosciences). The antibody titer is expressed as sbp x 10^{-3}/ml, calculated as previously described in detail[11].

Complement-dependent cytotoxicity.

DT6606 or K8484 cells were seeded in a 96-well plate (5 x 10^3/well) in DMEM-1% FBS overnight, for adhesion. Cells were washed with warm PBS and incubated with sera diluted in PBS (1:50) for 1h at 4°C, washed again, followed by incubation with fresh reconstituted rabbit complement (Low-Tox rabbit complement from Cederlane) diluted 1:25 in PBS for 1h at 37°C. Lysis was evaluated with the CytoTox 96 Non-Radioactive Cytotoxicity Assay (Promega). Lysis buffer was added to cells 45 min prior to centrifugation in order to obtain the maximum release of lactate dehydrogenase (LDH), while cells without serum and complement were used as a measure of spontaneous release of LDH. Plates were centrifuged at 250 x *g* for 4 minutes and 50 µL of supernatant was transferred to the enzymatic assay plate and incubated with 50 µL of substrate Mix for 30 min at room temperature in the dark. Stop solution (50µL) was added to each well and absorbance was recorded at 490 nm with a plate reader. An LDH positive control was added in new wells of each plate and all tests were performed in triplicate. The percentage of specific lysis was calculated using the following formula:

% cytotoxicity = [(Experimental-Target spontaneous) / (Target maximum-Target spontaneous)] x 100

IFN-γ Elispot assay.

Mouse lymph node and spleen cells were evaluated to determine the presence of T cells able to secrete IFN-γ in response to rENO1 or DT6606 cells, *ex-vivo* or after 1 week of *in vitro* culture in the presence of 10μg/ml of rENO1. Nitrocellulose plates (Millipore, Milan, Italy) were coated with anti-IFN-γ capture mAb (mIFN-γ kit by BD) overnight at 4 °C. T cells from lymph nodes and spleens *ex-vivo,* or recovered from a 1 week culture were stimulated with DT6606 cells (1:10 = S:E) or rENO1, for 40 h at 37 °C. T cells were seeded at 3 x 10^5 cells/well and all conditions were carried out in quadruplicate. Plates were then developed as indicated by the manufacturer using AEC (Sigma-Aldrich) substrate, and spots were quantified with the microplated reader along with a computer-assisted image analysis system (AID, Amplifon, Milan, Italy). The number of spots was calculated by subtracting the number of spots in medium only (background) from that in the presence of stimuli.

Flow cytometry.

Mouse MDSC were analyzed by staining whole blood after red cell lysis with 0.83% NH_4Cl-0.1% KHCO3-0.04% EDTA buffer and washing with PBS-0.2% BSA-0.01% NaN_3. This was followed, after blocking nonspecific sites, by incubation with mAbs from Biolegend: anti-CD16/CD32 mAb, anti-CD11b and anti-Gr1. Mouse PBMC- isolated by Ficoll centrifugation- were washed with PBS-0.2% BSA-0.01% NaN_3, stained with CD4 and CD25 mAbs (all from Biolegend), and subsequently fixed and permeabilized with Fixation and Permabilization solution (eBiosciences) for 30' at 4°C. After washing with Permeabilization buffer, cells were incubated for 30 min with FoxP3 and RoRγt mAbs (both from eBiosciences). Spleen cells (2x10^6/ml) from control or *ENO1*-vaccinated mice were stimulated with PMA (50 ng/ml) and Ionomycin (2 μg/ml) in the presence of the intracellular protein transport inhibitor brefeldin A (Sigma) *ex vivo* or after 1 week of culture in the presence of rENO1. Cells were harvested 5 h later, labeled with a CD4 mAb, and subsequently fixed with a 2% paraformaldehyde solution.

Cells were permeabilized using PBS-0.2% BSA-0.5% saponin and subsequently incubated for 30 min with mAbs specific for TNF-α, IFN-γ and IL-17 (all from BD or Biolegend). All flow cytometry data were acquired on a FACSCalibur (BD) and analyzed using FlowJo (Tree Star) or CellQuest Software (BD).

Histology.

Pancreas, spleen, liver and lungs from control and *ENO1*-vaccinated mice were sampled at the indicated times, fixed in formalin and subsequently paraffin-embedded. We quantified the percentage of transformed ducts compared to normal ducts on histological sections from H&E sections of the pancreas, according to the criteria previously established [8].

For immunohistochemical analysis, slides were subjected to microwaving for 20 min in 10 mmol/L of citrate buffer (pH 8.0 for nuclear antigens; pH 6.0 for other antigens). Immunostaining was performed using the avidin biotin peroxidase complex method or detected using the Dako Envision Plus Rabbit Polymer (K4033) and a semiautomated immunostainer (DAKO, Carpinteria, CA, USA or Ventana Systems, Tucson, AZ, USA). Primary antibody used was a rat anti-mouse FoxP3 1:50 (eBiosciences) and a rat anti-mouse CD3 1:100 (Dako). Reactive T lymphocytes and Treg cells were quantified by measuring the percentages of $CD3^+$ and $FoxP3^+$ cells, respectively, among the total mononuclear cells infiltrating the neoplastic pancreatic glands.

Statistical analysis*.*

We used an unpaired two-tailed Student's t-test for all comparisons. Kaplan-Mayer survival curves were created with GraphPad Software (Prism 5), and evaluated with both the Log Rank Mantel-Cox and the Gehan-Breslow-Wilcoxon test.

Results

The ENO1 vaccine induces both an antibody and a cellular response.

PDA-prone KC mice were electroporated either with empty plasmid or human ENO1-encoding plasmid. The amount of antibodies able to bind recombinant human ENO1 (rENO1) was evaluated at 2 weeks after the last electroporation. Anti-ENO1 antibodies were significantly induced in *ENO1*-vaccinated KC mice, but not in those vaccinated with the empty vector (Figure 1A).

To evaluate the functional role of anti-ENO1 antibodies, we first analyzed the ability of sera from empty or *ENO1*-vaccinated mice to bind the cell surface of murine PDA cells by flow cytometry, by measuring their binding potential (Figure 1B-D). Despite a weak cell decoration also being observed with sera from untreated mice, those from *ENO1*-vaccinated mice displayed higher serum binding potential (Figure 1B) and a significantly higher ability to mediate complement-dependent killing of both murine PDA K8484 and DT6606 cells (Figure 1D).

Spleen and lymph node cells from untreated, empty-vaccinated, and *ENO1*-vaccinated mice were collected 2 weeks after the final vaccination, and their ability to secrete IFN-γ was assessed in an Elispot assay, both *ex vivo* and after 7 days of *in vitro* re-stimulation with the rENO1. *Ex vivo* splenocytes from untreated and empty-vaccinated control mice (white and gray bars) displayed few specific spots when stimulated with rENO1 (Figure 2B, C). In contrast, *ex vivo* T cells from *ENO1*-vaccinated mice (black bars) displayed a significantly higher number of IFN-γ-secreting cells in response to rENO1 (Figure 2B), which increased three-fold after the *in vitro* rENO1 re-stimulation (Figure 2D). When DT6606 cells were used for stimulation, only rENO1 re-stimulated T cells from *ENO1*-vaccinated mice specifically secreted IFN-γ (Figure 1E). No IFN-γ-secreting cells appeared when DT6606 cells were pre-incubated with an anti-MHC class I antibody. Similar results were obtained with lymph node cells (data not shown).

ENO1 DNA vaccine prolongs mouse survival.

As electroporation of human ENO1-encoding plasmid induces both cellular and antibody-mediated immune reactions, the therapeutic efficacy of this response was evaluated. As shown in Figure 3 (A, B), almost all KC mice displayed transformed foci in the pancreas at the moment of the first electroporation. Their number increased until the tumor mass reached 85-100 % of the pancreas and 50% of mice died around 336 days of age due to the presence of large tumors (Figure 3C). The vaccination with empty vector slightly prolonged the median of survival by 56 days (p=0.9, Log-rank Mantel-Cox test). In *ENO1*-vaccinated mice, the median survival is extended by 140 days (50% of mice died around 474 days, p=0.033 vs untreated mice, Log-rank Mantel-Cox test) (Figure 3C), which amounts to more than one-third of their life expectancy. Despite the slight increase induced by the unspecific vaccination and electroporation, the ENO1 vaccine significantly prolonged the survival by a further 82 days (p=0.036 vs empty-vaccinated mice, Log-rank Mantel-Cox test).

Even the survival of the double-mutated KPC mice, whose faster tumor progression is evident from their shorter median survival (203 days compared to 336 days of KC), is prolonged by 42 days (20% of life expectancy; p=0.034 vs untreated mice and p=0.025 vs empty-vaccinated mice, Log-rank Mantel-Cox test) in *ENO1*-vaccinated mice but not in empty-vaccinated mice (50% of mice died around 160 days; p=0.25 vs untreated mice, Log-rank Mantel-Cox test) (Figure 3D).

Because of the small number of available KPC mice, histological and immunological studies were conducted on KC mice only. Histological analysis performed at 24 and 36 weeks of age with randomly vaccinated mice (n = 5 per group) confirmed the ability of the *ENO1* vaccine, and to a lesser extent, electroporation with the empty plasmid, to reduce the percentage of transformed ducts compared to control mice. At 24 weeks, while untreated KC mice displayed 58% of already transformed pancreatic ducts, those empty-vaccinated or those receiving *ENO1* vaccine displayed only 18 and 25.5%, respectively (Figure 3E). At 36 weeks, ducts were shown to be transformed in 85% of the pancreas of untreated mice and 56% in those empty-vaccinated, compared with only 40% in those *ENO1*-vaccinated (Figure 3F): two of these mice displayed an almost normal pancreas,

suggesting a complete recovery.

ENO1 DNA vaccine inhibits Myeloid-Derived Suppressor Cell and Treg expansion and promotes the Th17 response.

As myeloid-derived suppressor cells (MSDC) and regulatory T cells (Treg) have been reported in KC mice [12], the effect of *ENO1*-DNA vaccination on these cell subsets was investigated. Compared to control mice at 12 weeks of age, there was a similar percentage of MSDC (white bars, Figure 4A, left panel) in the blood of empty-vaccinated mice (gray bars), which significantly decreased in *ENO1*-vaccinated mice (black bars), with an even more pronounced effect in Treg cells (Figure 4A right panel). The percentages of MSDC and Treg cells in *ENO1*-vaccinated mice then increased to those of control mice at 52 and 76 weeks (Figure 4A).

Immunohistochemical examination of pancreatic tissues from untreated mice shows a progressive increase of $FoxP3^+$ cells in transformed ducts from 3% at 4 weeks of age to 13% at 24 weeks and 19% at 36 weeks. Empty-vaccination did not alter this progress, whereas the *ENO1*-vaccine significantly diminished both the 24- and the 36-week percentages (Figures 4B-F). It will be seen that these two percentages are stable.

Compared to untreated and empty-vaccinated mice, in *ENO1*-vaccinated mice the percentage of Treg cells decreased in parallel with the increase of the percentage of cells expressing RoRγt, a transcriptional factor related to Th17 cells [13] (data not shown). This corresponded to an increased percentage of cells secreting IL-17 and TNF-α, two signature cytokines of Th17 cells [14], accompanied by an increase of IFN-γ secreting cells in $CD4^+$ spleen cells from *ENO1*-vaccinated mice (Figure 5A). After 7 days of in vitro re-stimulation, the percentage of IL-17, TNF-α, IFN-γ and IL-17/TNF-α secreting cells significantly increased even further (Figure 5B). Furthermore, we analyzed by immunohistochemistry the CD3 infiltrate into neoplastic foci from pancreas collected from untreated mice and mice vaccinated with empty or *ENO1*-expressing plasmids. As shown in figure 5 (panels C-F), the percentage of CD3 on total inflammatory cells in the neoplastic foci was significantly

higher in ENO1-vaccinated mice compared to that observed in empty-vaccinated or untreated mice.

These results suggest that only the *ENO1*-vaccination was able to induce specific Th17 cells in parallel, and to diminish the frequency of suppressor cells such as MDSC and Treg cells, and of note, to actively recruit CD3 cells into tumor.

Therapeutical ENO1 DNA vaccine significantly slows PDA progression.

To evaluate the effect of ENO1 vaccine in a setting closer to that applicable in patients lately diagnosed or chemo- and radio-resistant, we vaccinated mice at 32-36 weeks of age. Mice were sacrificed at 52 weeks of age to evaluate by histological analysis the percentage of transformed ducts compared to the normal ducts. Empty-vaccinated mice showed around 79% of transformed ducts compared to about 50% observed in the pancreas of ENO1-vaccinated mice (Figure 6A). Of note, despite the difference in the presence of transformed ducts is not statistically different, the mean of dimension of the largest tumor is strongly and significantly less in *ENO1*-vaccinated mice compared to that evaluated in empty-vaccinated mice (Figure 6B). These results suggest that even in a desperate attempt to tackle PDA when tumors are well established, *ENO1* vaccine seems to have efficacy in delay tumor progression.

Discussion

We have previously demonstrated that ENO1, a novel PDA-associated antigen, could be a promising therapeutic candidate owing to its ability to induce an integrated humoral and cellular response [5]. The few PDA-associated antigens (CEA, Kras, MUC1 and gastrin) that have already been tested in clinical trials have demonstrated to have no impact on survival [15]. This highlights the challenge to identify new and more significant immunogenic targets.

Here we show, for the first time, that a DNA vaccine coding for a ubiquitous protein significantly induces a specific immune response that prolongs survival in a mouse model of PDA. Despite ENO1 being widely expressed, we have previously demonstrated that normal cells, whose ENO1 levels are lower than those of tumor cells, are spared from antigen-specific killing [5].

In this study, LSL-$Kras^{G12D}$ mice crossed with Pdx-1-Cre mice (KC mice) were used to obtain the specific expression of mutated $Kras^{G12D}$ in pancreatic cells. Each tumor evolves from a background of genomic instability that gives rise to a polyclonal tumor whose physiopathological features are similar to those of human PDA [8]. Indeed, high resolution assessments of chromosomal content have previously indicated that non-reciprocal translocations were found in most neoplastic cells that were analyzed [16]. This, and similar models of GEM, have been used to address therapeutic issues, but have never been for as long as in our study. We show that *ENO1* DNA vaccination significantly prolongs survival from 336 to 474 days of age, the longest overall survival ever reported.

In this study we show that the *ENO1*-vaccinated mice displayed higher amount of serum anti-ENO1 IgG and notably, that they are able to bind the cell surface of murine PDA cells and induce their killing by complement-dependent cytotoxicity, which has been proposed as an effector mechanism of anti-tumor immunity [17, 18]. Anti-ENO1 antibody induction correlates with the increase of ENO1-specific Th1 and Th17 T cells. The latter, in particular, may be crucially important in helping B cells to produce a pronounced amount of antibodies with

preferential isotype class switching to IgG1, IgG2a, IgG2b, and IgG3 [19], and IFN-γ to IgG2a [20]. Accordingly, we have documented a strong increase of T lymphocytes that infiltrate tumor area in ENO1 vaccinated mice. We are currently investigating other anti-tumor mechanisms dependent on anti-ENO1 IgG, specially after the important demonstration by Guo *et al*. that, in addition to surface molecules, proteins hidden within cells can also be attacked by antibodies [21]. Another possible role is the inhibition of migration of pancreatic tumor cells or MDSC into the tumor through the ENO1-plasminogen pathway blockade [22, 23].

An additional important effect of *ENO1* vaccination is the significant decrease of MDSC and Treg cells. The massive secretion of IL-6 in the pancreas of *ENO1*-vaccinated mice (data not shown) may explain the increase of Th17 rather than FoxP3$^+$ cells [24]. Th 17 cells recruit neutrophils and eosinophils [25], also present in pancreatic tumor lesions from empty-vaccinated mice (data not shown), and this native immune response partly impeded tumor progression, particularly at the beginning; indeed, at 24 weeks of age, both empty and *ENO1*-vaccinated mice presented a lower percentage of transformed pancreatic ducts compared to untreated mice. However, only the combination of the innate and acquired immune responses induced by the *ENO1* vaccination was able to significantly delay the tumor progression. At 36 weeks of age, only *ENO1*-vaccinated mice showed the lower percentage of transformed pancreatic ducts, and two of these five mice displayed an almost entirely histologically-normal pancreas. Nevertheless, when suppressive immune cells restored percentages similar to those of the controls, progression was no longer counteracted and death ensued. It is however possible that repeated boosters are required, as for other antigens, to maintain the minimal antigen concentration necessary for the adequate effector activation. Thus, all studies aimed to limit suppressor cells by a combination of different strategies are highly applicable, and it is likely that a combined vaccination schedule or different settings might be more efficient. In a GEM model of lung adenocarcinoma, vaccination clearly stimulated specific T cells which soon disappeared; tumor growth, in parallel, was slower at the beginning but then became similar to that in control mice [26]. This also endorses the great potential of the vaccination even if researchers have still to work on the most effective combination and timing. The choice of xenogenic rather

than syngeneic antigen or other kind of vectors remains open: many studies have demonstrated that human TAA compared to the mouse ortholog, or viral vectors compared to plasmid vectors used to vaccinate tumor-bearing mice are more efficient in inducing tumor immunity as well as autoimmunity. Thus, xenogenic TAA or viral components aid the immune system in breaking tolerance or ignorance against a "self"-protein [27-29] _ENREF_27. In our case, we have previously demonstrated that PBMC from PDA patients specifically secreted IFNγ in response to the syngeneic recombinant protein, and here we show that mice vaccinated with the xenogenic protein produce antibodies against the syngeneic native protein.

Our results are however very promising. Few of the many new strategies seem to be effective in prolonging survival beyond 1 year [15], while the optimal adjuvant approach after resection is still unclear [30]. Together these findings suggest that *ENO1*-vaccination in resected PDA patients might increase the Th17 population and limit the expansion of the MDSC, leading to an effective immune response that tackles the recurrence. In addition, this observation endorses previous data on the effector role of Th17 cells in tumors [31-33] even if their specific contribution in PDA remains to be clarified.

DNA vaccines could be employed in pancreatic cancer as adjuvants to conventional treatments, in the management of minimal residual disease, and as a way of increasing the overall survival of the 80% of resected patients who always develop recurrences.

Increasing data indicate that chemo-immunotherapy may constitute a new strategy to control tumor progression [34]. The immune system, indeed, could be elicited in two ways by conventional therapies. Some therapeutic programs elicit specific cellular responses that render tumor-cell death immunogenic [35]. Other drugs may have side effects that stimulate the immune system through different mechanisms. Moreover, vaccination against cancer-specific antigens may sensitize a tumor to subsequent chemotherapy [34], and in this contest the ENO1 vaccine can be also applied to chemo-resistant PDA patients. Lastly, the chemotherapeutic drug gemcitabine [36, 37] (but not doxorubixin-cyclophosphamide [38]), eliminates MDSC [39], and cyclophosphamide eliminates Tregs [40], which constitute one of the main immunosuppressive factors in cancer as well tumor-

associated stromal cells, and several strategies targeting them are currently being explored [39, 41]. Very promising, indeed, is the therapeutical efficacy of ENO1 vaccine observed when the administration protocol started at 32-36 weeks of age. The right drug combination might transform our trend in significant results. Overall, present data indicate that it may be possible to design adjuvant therapies to elicit anti-ENO1 responses in resected patients to prevent recurrences, or to prolong survival of untreatable patients.

Acknowledgements

We would like to thank Dr A. Amedei for scientific discussion, Dr. John Iliffe and Radhika Srinivasan for critically reading the manuscript, and M-S. Scalzo and R. Curto for technical help.

Figure Legends

Figure 1. Electroporation of human ENO1-encoding plasmid elicits antibodies to human and mouse ENO1. A. Anti-ENO1 IgG was quantified by ELISA in sera from untreated (white bars) and empty (gray bars) or *ENO1*-plasmid (black bars) vaccinated mice after three rounds of vaccination. Data are represented as mean ± SEM. B. Serum binding potential evaluated by flow cytometry with empty or *ENO1*-vaccinated mouse sera collected 2 weeks after the final vaccination. Values are expressed as mean x 10^{-3} ± SEM from 8-10 mice. *values from *ENO1*-vaccinated mice are significantly different from those of empty-vaccinated mice. C. Representative staining of murine DT6606 PDA cells with sera from empty or *ENO1*-vaccinated mice individually tested. Open profiles, cells stained with secondary antibody alone; solid black profiles, cells stained with sera from mice vaccinated with empty (left panel) or *ENO1* (right panel) plasmids. Two representative stainings are shown. D. Complement-dependent cytotoxicity of K8484 and DT6606 cells with sera from empty or *ENO1*-vaccinated mice, individually tested. The box-graphs include single % of lysis ± SEM, while the horizontal bars represent the median for each group of sera. * $p< 0.05$ and *** $p< 0.0001$ values from *ENO1*-vaccinated mice are significantly different from those of empty-vaccinated mice

Figure 2. ENO1- vaccine elicits cellular responses to human and mouse ENO1. Spleen cells from untreated mice (white bars), empty plasmid (gray bars) or *ENO1*-plasmid -vaccinated (black bars) mice were stimulated in Elispot plate with rENO1 (A, C) or DT6606 cells (B, D) *ex-vivo* (A, B) or after 7 days of stimulation with rENO1 (C, D). DT6606 cells were either pre-incubated or not with anti-MHC class I mAb (D). T cells cultured with medium alone are shown as light gray bars. The numbers in the graph represent the mean no. of specific spots subtracted from that of the background. All conditions were in quadruplicate. One of three independent experiments is shown, and results are expressed as mean ± SEM, $n = 2$ for each group. * $P < 0.05$, *** $P < 0.0001$ values compared to untreated mice and §§ $P < 0.001$, §§§ $P < 0.0001$ values compared to empty-vaccinated mice.

Figure 3. *ENO1* vaccine significantly prolongs the survival of KC and KPC mice. A, B. From 4 weeks of age, KC mice spontaneously develop PDA that histologically progresses from PanIN to carcinoma in situ. C, D. Kaplan-Meier analysis of survival of untreated and vaccinated with empty or human *ENO1* coding plasmid KC mice (C) and KPC mice (D) monitored until their death. E. Percentage of transformed ducts in KC mice untreated or vaccinated with empty or *ENO1*-DNA. ** $P < 0.001$ values compared to untreated mice.

Figure 4. *ENO1*-vaccination decreases MDSC and $FoxP3^+$ cells. A. Left panel: Whole blood from untreated (white bars), empty-vaccinated (gray bars) and *ENO1*-vaccinated (black bars) mice was stained after red blood cell lysis with anti-CD11b and anti-GR1 mAbs, and directly acquired with a FACSCalibur. The percentage of double positive cells from individual mice is reported as mean ± SEM; *n* = 4-8 per group. Right panel: the presence of FoxP3 transcriptional factor was assessed in PBMC from untreated (white bars), empty-vaccinated (gray bars) and *ENO1*-vaccinated (black bars) mice. The percentage of positive cells between total $CD4^+/CD25^+$ cells evaluated in each single mouse is reported as mean ± SEM; *n* = 4-8 per group. B. Quantification of $FoxP3^+$ cells in transformed pancreatic ducts (n=5 for each group). C-F. Pancreases from empty and *ENO1*-vaccinated mice sacrificed at 24 (C, D) and 36 (E, F) weeks of age respectively were stained with the anti-FoxP3 Ab. ** $P < 0.01$ values significantly different from untreated mice and §§ $P < 0.001$, $^{§§§}P < 0.0001$ values significantly different from empty vaccinated mice.

Figure 5. ENO1 vaccination increases IL17 production. Spleen cells from untreated (white bars), empty-vaccinated (gray bars) and *ENO1*-vaccinated (black bars) mice were stimulated with PMA and Ionomycin overnight in the presence of brefeldin A, *ex vivo* (A) and after *in vitro* stimulation with rENO1 for 7 days (B), then stained for intracellular cytokines. The percentage of positive cells in total $CD4^+$ cells evaluated in each single mouse is represented as mean ± SEM; *n* = 6 per group. * $P < 0.05$ values significantly different from untreated mice and § $P < 0.05$ values significantly different from empty vaccinated mice. (C) Quantification of $CD3^+$ cells in transformed pancreatic ducts (n=6-8 for each group). D-F. Pancreases from untreated (D), empty (E) and *ENO1*-vaccinated (F) mice sacrificed at 24 weeks of age respectively

were stained with the anti-CD3 Ab. * $P < 0.05$ values significantly different from untreated mice; §§ $P < 0.01$ values significantly different from empty vaccinated mice.

Figure 6. Late *ENO1* vaccination significantly delays PDA progression. KC mice were vaccinated starting at 32 weeks of age when pancreatic ductal adenocarcinoma were well established, every 3 weeks for a total of three rounds. A. Percentage of transformed ducts in KC mice vaccinated with empty or *ENO1*-DNA (n=7-8 for each group). B. Quantification of the largest focus (mm) in the pancreas of mice vaccinated with empty or *ENO1*-DNA (n=7-8 for each group). §§§ $P < 0.0001$ values compared to empty vaccinated mice.

References

1. Jemal A, Siegel R, Ward E, et al. Cancer statistics, 2008. CA Cancer J Clin 2008;58:71-96.

2. Omura N, Goggins M. Epigenetics and epigenetic alterations in pancreatic cancer. Int J Clin Exp Pathol 2009;2:310-26.

3. Tomaino B, Cappello P, Capello M, et al. Autoantibody signature in human ductal pancreatic adenocarcinoma. J Proteome Res 2007;6:4025-31.

4. Tomaino B, Cappello P, Capello M, et al. Circulating autoantibodies to phosphorylated alpha-enolase are a hallmark of pancreatic cancer. J Proteome Res.

5. Cappello P, Tomaino B, Chiarle R, et al. An integrated humoral and cellular response is elicited in pancreatic cancer by alpha-enolase, a novel pancreatic ductal adenocarcinoma-associated antigen. Int J Cancer 2009;125:639-48.

6. Capello M, Ferri-Borgogno S, Cappello P, et al. alpha-enolase: a promising therapeutic and diagnostic tumor target. Febs J;278:1064-74.

7. Pancholi V. Multifunctional alpha-enolase: its role in diseases. Cell Mol Life Sci 2001;58:902-20.

8. Hingorani SR, Petricoin EF, Maitra A, et al. Preinvasive and invasive ductal pancreatic cancer and its early detection in the mouse. Cancer Cell 2003;4:437-50.

9. Hruban RH, Adsay NV, Albores-Saavedra J, et al. Pathology of genetically engineered mouse models of pancreatic exocrine cancer: consensus report and recommendations. Cancer Res 2006;66:95-106.

10. Giallongo A, Feo S, Moore R, et al. Molecular cloning and nucleotide sequence of a full-length cDNA for human alpha enolase. Proc Natl Acad Sci U S A 1986;83:6741-5.

11. Giovarelli M, Cappello P, Forni G, et al. Tumor rejection and immune memory elicited by locally released LEC chemokine are associated with an impressive recruitment of APCs, lymphocytes, and granulocytes. J Immunol 2000;164:3200-6.

12. Clark CE, Hingorani SR, Mick R, et al. Dynamics of the immune reaction to pancreatic cancer from inception to invasion. Cancer Res 2007;67:9518-27.

13. Martinez GJ, Nurieva RI, Yang XO, et al. Regulation and function of proinflammatory TH17 cells. Ann N Y Acad Sci 2008;1143:188-211.

14. Kryczek I, Banerjee M, Cheng P, et al. Phenotype, distribution, generation, and functional and clinical relevance of Th17 cells in the human tumor environments. Blood 2009;114:1141-9.

15. Laheru D, Jaffee EM. Immunotherapy for pancreatic cancer - science driving clinical progress. Nat Rev Cancer 2005;5:459-67.

16. Hingorani SR, Wang L, Multani AS, et al. Trp53R172H and KrasG12D cooperate to promote chromosomal instability and widely metastatic pancreatic ductal adenocarcinoma in mice. Cancer Cell 2005;7:469-83.

17. Weiner LM, Murray JC, Shuptrine CW. Antibody-based immunotherapy of cancer. Cell 2012;148:1081-4.

18. Shuptrine CW, Surana R, Weiner LM. Monoclonal antibodies for the treatment of cancer. Semin Cancer Biol 2012;22:3-13.

19. Mitsdoerffer M, Lee Y, Jager A, et al. Proinflammatory T helper type 17 cells are effective B-cell helpers. Proc Natl Acad Sci U S A;107:14292-7.

20. Hasbold J, Hong JS, Kehry MR, et al. Integrating signals from IFN-gamma and IL-4 by B cells: positive and negative effects on CD40 ligand-induced proliferation, survival, and division-linked isotype switching to IgG1, IgE, and IgG2a. J Immunol 1999;163:4175-81.

21. Guo K, Li J, Tang JP, et al. Targeting intracellular oncoproteins with antibody therapy or vaccination. Sci Transl Med;3:99ra85.

22. Lopez-Alemany R, Longstaff C, Hawley S, et al. Inhibition of cell surface mediated plasminogen activation by a monoclonal antibody against alpha-Enolase. Am J Hematol 2003;72:234-42.

23. Wygrecka M, Marsh LM, Morty RE, et al. Enolase-1 promotes plasminogen-mediated recruitment of monocytes to the acutely inflamed lung. Blood 2009;113:5588-98.

24. Gnerlich JL, Mitchem JB, Weir JS, et al. Induction of Th17 cells in the tumor microenvironment improves survival in a murine model of pancreatic cancer. J Immunol;185:4063-71.

25. Fujita K, Ewing CM, Sokoll LJ, et al. Cytokine profiling of prostatic fluid from cancerous prostate glands identifies cytokines associated with extent of tumor and inflammation. Prostate 2008;68:872-82.

26. DuPage M, Cheung AF, Mazumdar C, et al. Endogenous T cell responses to antigens expressed in lung adenocarcinomas delay malignant tumor progression. Cancer Cell;19:72-85.

27. Weber LW, Bowne WB, Wolchok JD, et al. Tumor immunity and autoimmunity induced by immunization with homologous DNA. J Clin Invest 1998;102:1258-64.

28. Bowne WB, Srinivasan R, Wolchok JD, et al. Coupling and uncoupling of tumor immunity and autoimmunity. J Exp Med 1999;190:1717-22.

29. Overwijk WW, Tsung A, Irvine KR, et al. gp100/pmel 17 is a murine tumor rejection antigen: induction of "self"-reactive, tumoricidal T cells using high-affinity, altered peptide ligand. J Exp Med 1998;188:277-86.

30. Li J, Merl MY, Chabot J, et al. Updates of adjuvant therapy in pancreatic cancer: where are we and where are we going? Highlights from the "2010 ASCO Annual Meeting". Chicago, IL, USA. June 4-8, 2010. Jop;11:310-2.

31. Kryczek I, Wei S, Szeliga W, et al. Endogenous IL-17 contributes to reduced tumor growth and metastasis. Blood 2009;114:357-9.

32. Martin-Orozco N, Muranski P, Chung Y, et al. T helper 17 cells promote cytotoxic T cell activation in tumor immunity. Immunity 2009;31:787-98.

33. Zou W, Restifo NP. T(H)17 cells in tumour immunity and immunotherapy. Nat Rev Immunol;10:248-56.

34. Zitvogel L, Apetoh L, Ghiringhelli F, et al. Immunological aspects of cancer chemotherapy. Nat Rev Immunol 2008;8:59-73.

35. Kroemer G, Zitvogel L. Death, danger, and immunity: an infernal trio. Immunol Rev 2007;220:5-7.

36. Suzuki E, Kapoor V, Jassar AS, et al. Gemcitabine selectively eliminates splenic Gr-1+/CD11b+ myeloid suppressor cells in tumor-bearing animals and enhances antitumor immune activity. Clin Cancer Res 2005;11:6713-21.

37. Ko HJ, Kim YJ, Kim YS, et al. A combination of chemoimmunotherapies can efficiently break self-tolerance and induce antitumor immunity in a tolerogenic murine tumor model. Cancer Res 2007;67:7477-86.

38. Diaz-Montero CM, Salem ML, Nishimura MI, et al. Increased circulating myeloid-derived suppressor cells correlate with clinical cancer stage, metastatic tumor burden, and doxorubicin-cyclophosphamide chemotherapy. Cancer Immunol Immunother 2009;58:49-59.

39. Gabrilovich DI, Nagaraj S. Myeloid-derived suppressor cells as regulators of the immune system. Nat Rev Immunol 2009;9:162-74.

40. Sistigu A, Viaud S, Chaput N, et al. Immunomodulatory effects of cyclophosphamide and implementations for vaccine design. Semin Immunopathol;33:369-83.

41. Kraman M, Bambrough PJ, Arnold JN, et al. Suppression of antitumor immunity by stromal cells expressing fibroblast activation protein-alpha. Science;330:827-30.

Figure 1

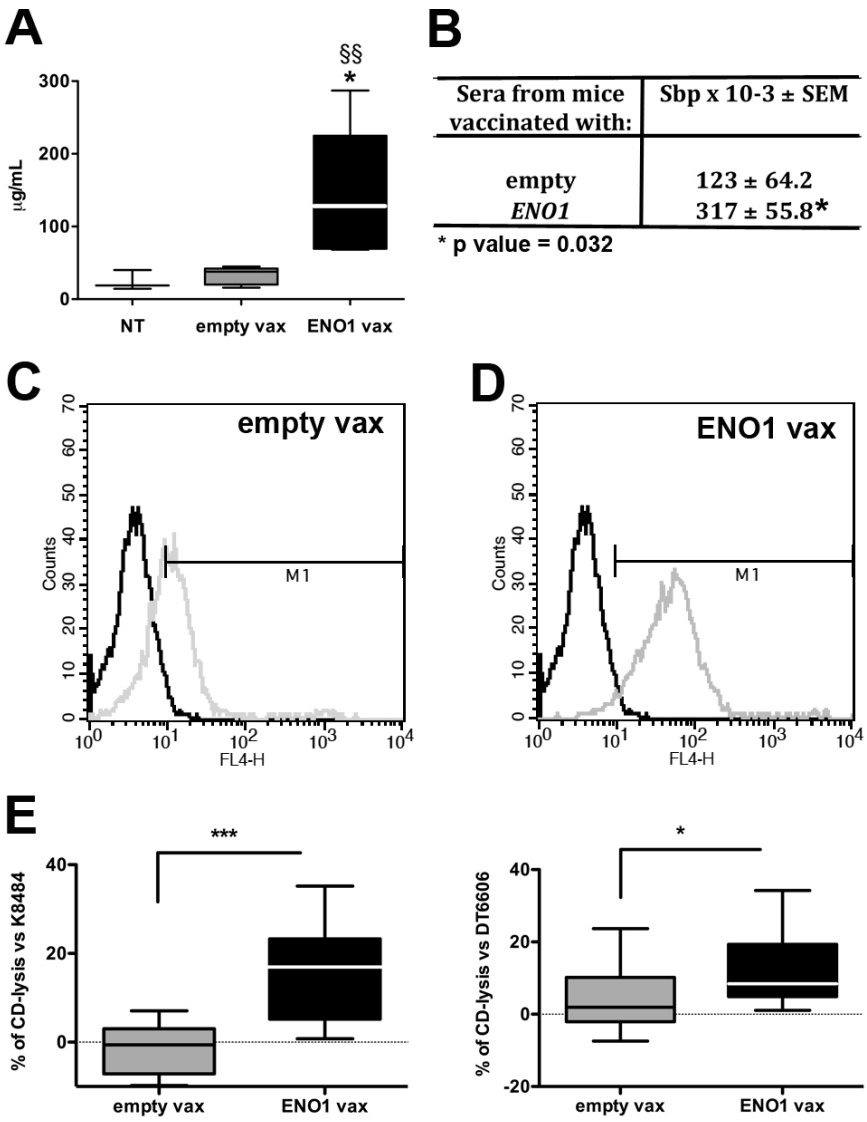
A
§§
*
300
200
100
0
µg/mL
NT
empty vax
ENO1 vax
B
Sera from mice vaccinated with:
Sbp x 10-3 ± SEM
empty
123 ± 64.2
ENO1
317 ± 55.8*
* p value = 0.032
C
empty vax
M1
Counts
FL4-H
D
ENO1 vax
M1
Counts
FL4-H
E
***
% of CD-lysis vs K8484
empty vax
ENO1 vax
*
% of CD-lysis vs DT6606
empty vax
ENO1 vax

Figure 2

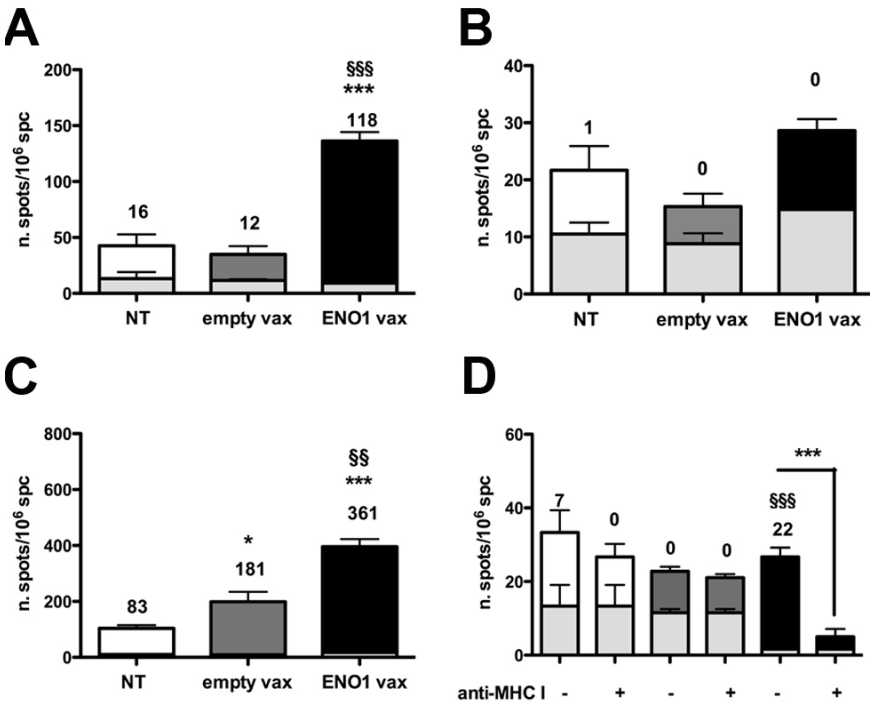
A
n. spots/10^6 spc
200
150
100
50
0
16
12
§§§
***
118
NT
empty vax
ENO1 vax
B
n. spots/10^6 spc
40
30
20
10
0
1
0
0
NT
empty vax
ENO1 vax
C
n. spots/10^6 spc
800
600
400
200
0
83
*
181
§§
***
361
NT
empty vax
ENO1 vax
D
n. spots/10^6 spc
60
40
20
0
7
0
0
0
§§§
22
***
anti-MHC I - + - + - +

Figure 3

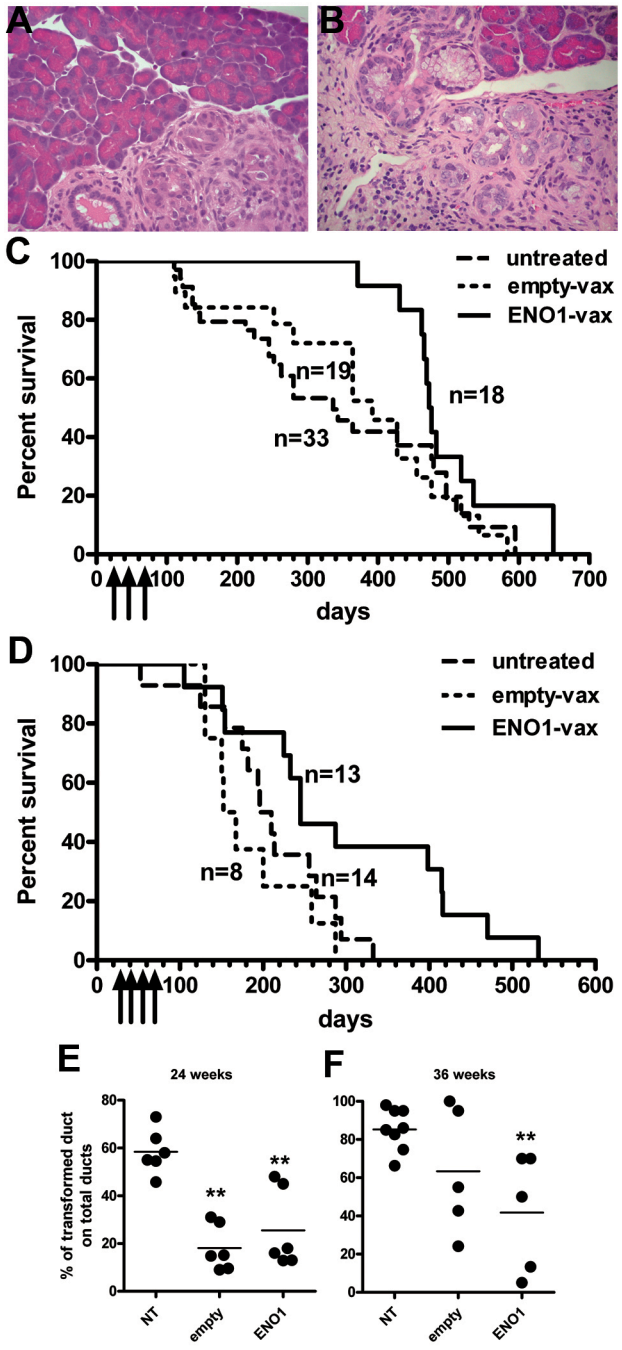
A
B
C
untreated
empty-vax
ENO1-vax
Percent survival
n=19
n=33
n=18
days
D
untreated
empty-vax
ENO1-vax
Percent survival
n=13
n=8
n=14
days
E
24 weeks
% of transformed duct on total ducts
**
**
NT
empty
ENO1
F
36 weeks
**
NT
empty
ENO1

Figure 4

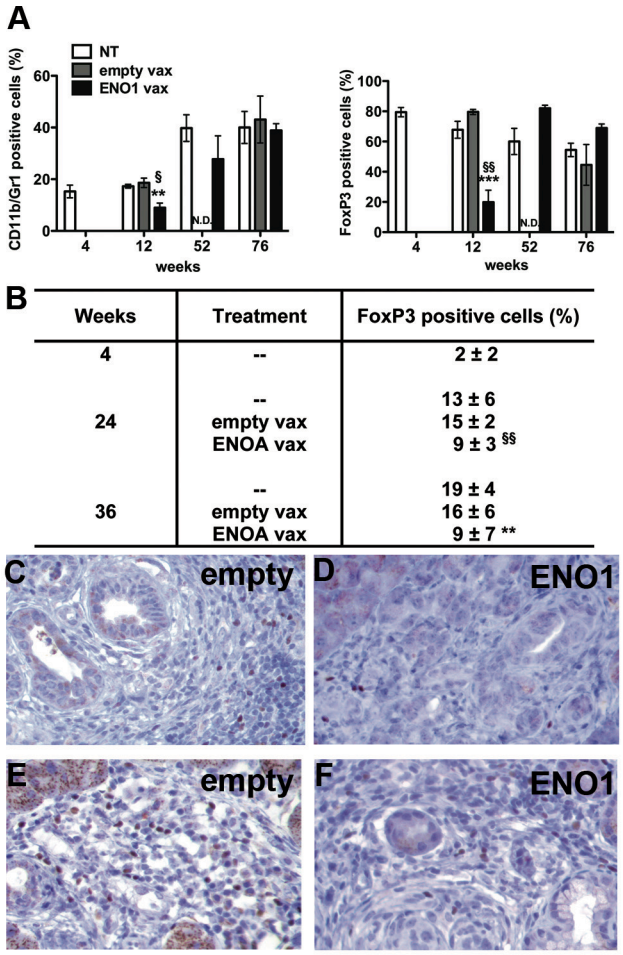

B

Weeks	Treatment	FoxP3 positive cells (%)
4	--	2 ± 2
24	--	13 ± 6
	empty vax	15 ± 2
	ENOA vax	9 ± 3 §§
36	--	19 ± 4
	empty vax	16 ± 6
	ENOA vax	9 ± 7 **

Figure 5

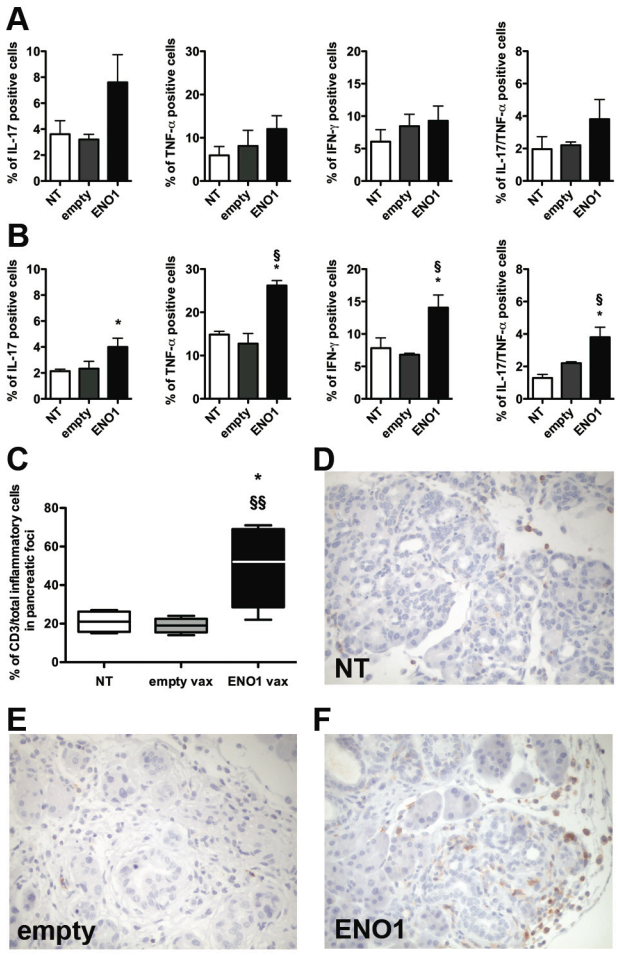
A
% of IL-17 positive cells
% of TNF-α positive cells
% of IFN-γ positive cells
% of IL-17/TNF-α positive cells
NT
empty
ENO1
B
*
§
C
% of CD3/total inflammatory cells in pancreatic foci
§§
NT
empty vax
ENO1 vax
D
NT
E
empty
F
ENO1

Figure 6

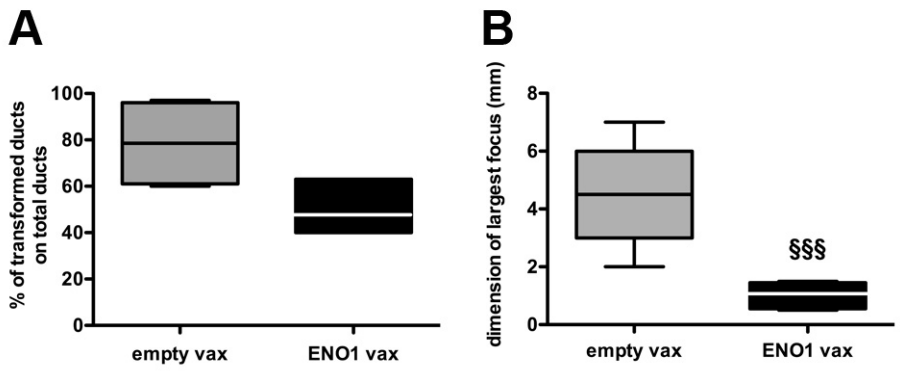
A
% of transformed ducts on total ducts
100
80
60
40
20
0
empty vax
ENO1 vax
B
dimension of largest focus (mm)
8
6
4
2
0
§§§
empty vax
ENO1 vax